Research Square

Preprints are preliminary reports that have not undergone peer review.
They should not be considered conclusive, used to inform clinical practice,
or referenced by the media as validated information.

Quantitative Systems Pharmacology Analysis of Amyloid Aggregation and Hippocampal Atrophy Trajectories in Alzheimer's Disease by APOE4 Genotype and Valiltramiprosate/ALZ-801 Treatment

John A. Hey

john.hey@alzheon.com

Alzheon, Inc

Hugo Geerts

Certara

Jean F. Schaefer

Alzheon, Inc

Shaina M. Short

Certara

Piet Graaf

Certara

Susan Abushakra

Alzheon, Inc

Aidan Power

Alzheon, Inc

Martin Tolar

Alzheon, Inc

Jeremy Y. Yu

Alzheon, Inc

Article

Keywords: ALZ-801, valiltramiprosate, Alzheimer's disease, APOE4, β-amyloid, oligomer, protofibril, hippocampal volume, quantitative systems pharmacology, SUVR

Posted Date: August 24th, 2026

DOI: https://doi.org/10.21203/rs.3.rs-10570608/v1

License: This work is licensed under a Creative Commons Attribution 4.0 International License.
Read Full License

Additional Declarations: No competing interests reported.

Nature Partners Journal (NPS) Systems Biology and Applications

(Original Research Article)

Quantitative Systems Pharmacology Analysis of Amyloid Aggregation and Hippocampal Atrophy Trajectories in Alzheimer's Disease by APOE4 Genotype and Valiltramiprosate/ALZ-801 Treatment

John A. Hey[1], Hugo Geerts[2], Jean F. Schaefer[1], Shaina M. Short[2], Piet van der Graaf[2], Susan Abushakra[1], Aidan Power[1], Martin Tolar[1] and Jeremy Y. Yu[1]

Corresponding author: Dr. John A. Hey, Alzheon, Inc., 111 Speen Street, Suite 306, Framingham, MA 01701, USA. Email: john.hey@alzheon.com

Affiliations: [1]Alzheon, Inc., Framingham, MA, USA; [2]Certara, Radnor, PA, USA

Funding: This research was funded by Alzheon, Inc.

Abstract words: 328

Figures: 10

Tables: 2

References: 68

Running title: QSP trajectories of Alzheimer's disease by APOE4 genotype and effects of valiltramiprosate

Key words: ALZ-801, valiltramiprosate, Alzheimer's disease, APOE4, β-amyloid, oligomer, protofibril, hippocampal volume, quantitative systems pharmacology, SUVR

Abbreviations:

Aβ, β-Amyloid

AD, Alzheimer's Disease

ADNI, Alzheimer's Disease Neuroimaging Initiative

APOE, Apolipoprotein E

APP, Amyloid Precursor Protein

ARIA, Amyloid-related Imaging Abnormalities

ARIA-E, Amyloid-related Imaging Abnormalities (Edematous)

ARIA-H, Amyloid-related Imaging Abnormalities (Hemorrhagic)

AUC, Area under the Curve

BACE, Beta Amyloid Cleaving Enzyme

BBB, Blood-Brain Barrier

BCSFB, Blood-Cerebro-Spinal Fluid Barrier

BID, *bis in die*

CNS, Central Nervous System

CSF, Cerebro-Spinal Fluid

DAM, Disease-associated Microglia

DTI, Diffusion Tensor Imaging

ISF, Interstitial Fluid

MCI, Mild Cognitive Impairment

MOA, Mechanism of Action

MRI, Magnetic Resonance Imaging

PBPK, Physiologically Based Pharmacokinetics

PK, Pharmacokinetics

QSP, Quantitative Systems Pharmacology

SUVR, Standardized Uptake Value Ratio

vMRI, Volumetric Magnetic Resonance Imaging

ABSTRACT

Apolipoprotein E4 (APOE4) is a major risk factor for Alzheimer's disease (AD). Valiltramiprosate/ALZ-801, an oral inhibitor of β-amyloid (Aβ) oligomer formation, was evaluated in APOE4/4 subjects with early AD in the APOLLOE4 Phase 3 trial. We used quantitative systems pharmacology (QSP) to characterize AD trajectories by APOE genotype and assess the effects of valiltramiprosate treatment. An existing QSP model of Aβ aggregation in AD was extended to incorporate APOE4 genotypes and a hippocampal atrophy readout based on hippocampal volume (HV), calibrated with observational and interventional data from lecanemab and donanemab studies. Valiltramiprosate's anti-Aβ oligomer and APOE4 structure-corrector pharmacology was simulated over 2-10 years of treatment. Model predictions were validated against the plasma Aβ42/Aβ40 results from the valiltramiprosate Phase 2 study and HV outcomes from APOLLOE4. APOE genotype altered the natural trajectory of Aβ aggregation, with APOE4/4 associated with earlier onset and faster pathology, consistent with a gene-dose effect (APOE4/4 >> APOE3/4 > APOE3/3). Valiltramiprosate 265 mg administered orally twice daily increased the plasma Aβ42/Aβ40 ratio and CSF Aβ42, reduced oligomers and protofibrils, and had minimal effects on plaques. Long-term modeled treatment with valiltramiprosate prevented aggregation and shifted Aβ toward monomers. The QSP analysis was supported by Phase 2 plasma Aβ42/Aβ40 findings and was consistent with Phase 3 results, indicating greater brain volumetric benefit in APOE4/4 subjects with Mild Cognitive Impairment (MCI) than in those with mild AD. The magnitude of valiltramiprosate's effects depended on age, genotype, and disease stage, and was substantially differentiated from anti-amyloid antibody monotherapy with lecanemab or donanemab. A measurable APOE4 structure-corrector effect was observed in APOE4 carriers; however, anti-Aβ oligomer pharmacology accounted for most of valiltramiprosate's effects on

fluid biomarkers and hippocampal atrophy trajectories over time in AD. This enhanced Aβ aggregation and HV QSP model enables evaluation of therapeutic interventions across APOE genotypes. These findings support greater benefit of oral valiltramiprosate in early AD, particularly MCI, and suggest potential utility as preventive therapy in presymptomatic AD.

1. Introduction

Alzheimer's disease (AD) is the most common form of dementia, comprising over two-thirds of cases in people aged 65 and older. In the United States alone, approximately 7.2 million people have AD dementia, with an additional 20 million expected to have preclinical AD by 2025 (1, 2). Fewer than 5% of cases result from inherited mutations in amyloid precursor protein (APP), presenilin 1, or presenilin 2, causing early onset; most cases develop after age 65. AD is marked by progressive neurodegeneration and brain atrophy, especially in the hippocampus (3). Key pathological features include the accumulation of extracellular β-amyloid (Aβ) plaques and intracellular neurofibrillary tangles, which are detected using biomarker assays like CSF Aβ42, plasma Aβ42/Aβ40 ratio, pTau-217/Aβ42 ratio, and amyloid and tau PET scans for disease diagnosis, severity classification, and as surrogate endpoints in clinical trials.

Major advancements have been made in the understanding of AD pathogenesis, particularly regarding the amyloid cascade and the downstream tau pathway. Current research indicates that soluble aggregates of Aβ (known as oligomers), rather than monomers or plaques, play a pivotal role in driving AD pathogenesis and progression (4-5). The highly neurotoxic Aβ oligomers result in neuronal loss and cerebral atrophy (6). Furthermore, these oligomers can instigate tau pathology, which contributes to disease advancement in later stages (7, 8). Presently, three anti-amyloid antibodies (aducanumab, lecanemab, and donanemab) have obtained regulatory

approval for AD therapy (9-11). Additionally, a small-molecule oral anti-oligomer agent, valiltramiprosate (also known as ALZ-801), has shown favorable clinical and volumetric brain outcomes in APOE4/4 homozygotes with Mild Cognitive Impairment (MCI) in a Phase 3 trial (12-14). These findings provide clinical proof-of-concept supporting the critical involvement of Aβ oligomers in AD pathogenesis and validate their value as a therapeutic target.

The risk, onset, and progression of late-onset AD are shaped by multiple genetic, environmental, and lifestyle factors. Among these, the ε4 allele of apolipoprotein E (APOE4) stands out as the most influential genetic contributor and is considered the strongest risk factor after age (15-16). Possessing one copy of the APOE4 allele increases the risk by threefold, while having two copies raises it by approximately 10-12 times. In contrast, the APOE3 allele seems not to affect risk, and APOE2 offers some protection. Earlier studies showed that patients with two copies of APOE4 allele (homozygotes) developed AD symptoms approximately six years earlier (at ~66 years old) compared to those with one copy or none, while individuals with one copy (heterozygotes) showed a smaller shift, developing symptoms at around age 70 compared to 72 for non-carriers (17). More recent work by Fortea et al. (16) confirmed a dose-dependent effect of APOE4 on lowering CSF Aβ42 levels, with the greatest reduction seen in APOE4/4 individuals, followed by APOE3/4, and then APOE3/3. This suggests that AD in APOE4/4 homozygotes may represent a distinct subtype, marked by a semi-dominant genetic form and nearly complete manifestation of AD pathology by age 65. Although the underlying disease mechanisms are shared across all APOE genotypes, those who are APOE4/4 homozygotes experience quicker onset and more aggressive progression than heterozygotes or non-carriers.

Hippocampal volume (HV), as measured by volumetric Magnetic Resonance Imaging (vMRI), has been proposed as both a pharmacodynamic outcome measure and a predictive marker

of disease progression to serve as an enrichment tool in AD clinical trials, as recommended by the Alzheimer's Disease Neuroimaging Initiative (ADNI) and the Food and Drug Administration (FDA) Critical Path Institute (18-21). The European Medicines Agency (22) further endorsed vMRI imaging outcomes for assessing disease modification in AD trials. Drawing on published data from 30 observational studies (n=13,187) and six placebo-controlled interventional trials involving four anti-amyloid agents (n≈8,000) with demonstrated clinical efficacy, we have assessed the potential utility of HV as a surrogate endpoint for predicting clinical benefit in disease-modification trials (14). Notably, significant correlations were observed between baseline HV and cognitive performance, as well as between hippocampal atrophy and cognitive decline over a period of one year or longer. Moreover, a strong linear correlation was identified between reduced hippocampal atrophy and attenuated cognitive decline in clinical trial settings, indicating that hippocampal atrophy serves as an early marker of AD closely associated with amyloid- and tau-related neurodegeneration and cognitive impairment. These findings highlight HV as a sensitive marker for forecasting clinical benefit in early-stage AD and emphasize the importance of hippocampal atrophy and neurodegeneration - core features of AD represented by the "N" component in the A/T/N classification system (23).

Valiltramiprosate is an oral, small-molecule, valine-conjugated prodrug of tramiprosate (4, 5, 12-14, 24-30). It works by inhibiting the formation of Aβ oligomers and is being studied as a potential treatment to slow or modify the progression of AD. Its late-stage clinical trials include a Phase 2 biomarker study in APOE4 carriers and a Phase 3 study in APOE4/4 homozygotes, along with long-term extension studies (12-14, 28-30).

After oral administration, valiltramiprosate quickly converts to tramiprosate, which then breaks down into its final active form, 3-sulfopropanoic acid (3-SPA; 27, 30, 31). Both

tramiprosate and 3-SPA act against Aβ oligomers, forming the primary mechanism of action (MOA) for valiltramiprosate (31-33). Both compounds readily enter the brain, with preclinical studies showing that their steady-state brain-to-plasma area-under-the-curve (AUC) ratio ranges from 40% to over 80% (24, 27, 31). Further confirmation of valiltramiprosate's activity in preventing Aβ oligomer formation was provided by Muramatsu et al. (34). Beyond their anti-amyloid effects, both tramiprosate and 3-SPA, the active components of valiltramiprosate, have been shown to correct the structure and function of the abnormal APOE4 protein, shifting it toward a normal APOE3-like form (35).

Although the APOLLOE4 Phase 3 trial in APOE4/4 homozygotes did not achieve its primary endpoint of cognitive slowing in the early AD population, valiltramiprosate demonstrated a statistically significant improvement in cognition (ΔADAS-Cog13 = -2.144, p = 0.041) and function (ΔCDR-SB = -0.646, p = 0.053) within the pre-specified MCI group (13, 14). In addition, valiltramiprosate consistently resulted in reduced hippocampal atrophy (-26%, p = 0.0042 in MCI) and showed favorable outcomes across other brain regions, including increased cortical thickness, greater whole brain volume, and less ventricular expansion (13, 14), suggesting substantial neuroprotective effects.

We previously developed a quantitative systems pharmacology (QSP) model for Aβ aggregation in APOE4 carrier and non-carrier AD, and utilized the model to characterize biomarker dynamics, the efficacy of anti-amyloid antibody therapies, and the incidence of amyloid-related imaging abnormalities-edema (ARIA-E) (36, 37). This model has also been used to evaluate the impact of valiltramiprosate on Aβ fluid biomarkers in a Phase 2 study (28). Building upon this foundation, the current study aimed to: 1) expand the QSP Aβ aggregation model by incorporating the APOE4 genotypes, specifically APOE4/4 and APOE3/4 vs. APOE3/3; 2)

develop a natural trajectory model of HV changes in AD based on APOE4 genotypes; and 3) predict the effects of valiltramiprosate on AD progression by Aβ biomarkers and HV across the APOE genotype groups. Once validated, this enhanced Aβ aggregation and HV QSP model can be used for assessment of therapeutic interventions (e.g., monotherapies and combination treatment scenarios with anti-amyloid antibodies) across the different APOE genotypes.

2. Methods

This work expanded an existing QSP Aβ aggregation model in AD (36, 37) by introducing the impact of APOE4 genotypes, specifically, APOE4/4 and APOE3/4 vs. APOE3/3, in order to predict the APOE4 genotype-specific natural trajectories of Aβ biomarker and HV changes in AD. Based on this enhanced QSP model, the effects of valiltramiprosate treatment were simulated in generic AD patients. The QSP model-predicted treatment effects were subsequently compared with the valiltramiprosate Phase 2 and Phase 3 clinical trial results as a form of validation. The overall workflow is illustrated in Figure 1.

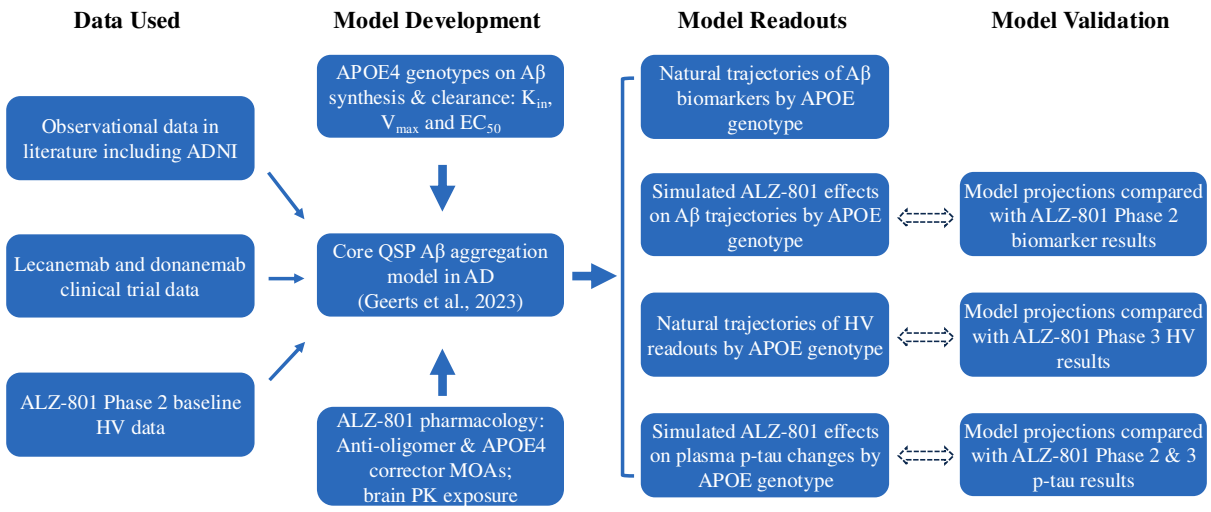


Figure 1. Overall workflow of APOE4 genotype-specific QSP model development. *The model development built off the previously published QSP Aβ aggregation model in AD (36, 37) by introducing the APOE4 genotype-specific effects on both Aβ production and clearance. Based on this enhanced Aβ aggregation model, an APOE4-genotype specific readout of the natural trajectory of hippocampal volume (HV) in AD was developed. The model was calibrated with both longitudinal observational and interventional (lecanemab and donanemab) data, as well as the valiltramiprosate (ALZ-801) Phase 2 baseline hippocampal volume data. The impact of valiltramiprosate was introduced to the model based on its anti-oligomer and APOE4 structure corrector MOAs and the steady state pharmacokinetic exposures in the brain. A derivative simulation of plasma p-tau changes following valiltramiprosate treatment was also conducted. The QSP model-predicted changes of plasma Aβ42/ Aβ40 ratio, HV and plasma p-tau levels were subsequently compared with the actual valiltramiprosate clinical trial results as a form of model validation.*

2.1 General Aβ aggregation model

The QSP Aβ aggregation model in APOE4 carrier vs. non-carrier AD was previously reported (36, 37). In brief, the model consists of a physiologically based pharmacokinetic (PBPK) model coupled to a mechanistic QSP model of Aβ aggregation. The PBPK model lumps peripheral tissues together but models explicitly lymph, plasma, four different cerebro-spinal fluid (CSF) and interstitial fluid (ISF) compartments including the blood-brain barrier (BBB) and the blood-CSF barrier (BCSFB). Conversely, by using the same principles, this model can be used to derive the level of peripheral biomarkers originating from the brain ISF, e.g., monomeric Aβ42 and Aβ40 in lumbar CSF and plasma. The mechanistic QSP model describes the synthesis of both Aβ species from APP, the enzymatic degradation of Aβ monomers by insulin-degrading enzyme or neprilysin, the aggregation of Aβ monomers into oligomers, protofibrils and plaques, and the clearance of oligomers, protofibrils and plaques by microglia. We defined monomers (n=1), oligomers (n=2-16) with molecular weights (MW) between 8 and 80 kDa, protofibrils (n=17-24) with MW >80 kDa (38) and plaques (n≥25). As monomeric Aβ can be synthesized in peripheral organs such as the liver (39), a synthesis process of free Aβ monomers was incorporated with the differential rate constant adjusted to align with the actual plasma levels of the Aβ monomers measured in longitudinal studies (40).

As described (36), this model allows for simulating the natural trajectory of amyloid biomarkers from birth onwards. The readouts include plasma Aβ42/Aβ40 ratio, CSF Aβ42, and standardized uptake value ratio (SUVR), which were calibrated with both longitudinal and interventional clinical studies. Important readouts of the model, which have impact on the subsequent prediction of HV, include the experimentally “inaccessible” soluble oligomers and protofibrils. Modeling the levels of soluble oligomers and protofibrils and insoluble plaques were constrained from postmortem biochemical studies in AD brains (41). The calculations of Aβ42

oligomers, protofibirils and SUVR are described below, with the latter based on the contributions of both soluble and insoluble Aβ aggregates. $A\beta42^{oligo}$, $A\beta42^{proto}$ and $A\beta42^{plaque}$ are weighted averages of oligomer levels (i.e., n-mer oligomer concentration * n), protofibrils, and plaques. The C1, C2, C3 and C4 parameters were derived from the optimal correlation between the simulated and clinically observed values from six anti-amyloid antibodies in the initial model (36). Additionally, the SUVR for florbetapir can be calculated in centiloids using the formula Amyloid (Cl)=183*SUVR-177 (42).

$$Oligomer_{weighted} = \sum_{i=2}^{i=16} Ab42_i * i \qquad \textit{Equation 1}$$

$$Protofibril_{weighted} \sum_{i=17}^{i=23} Ab42_i * i \qquad \textit{Equation 2}$$

$$SUVR_w = 1 + \frac{C_1\left(Ab42^{oligo} + Ab42^{proto} + C_2 * Ab42^{plaque}\right)^{C_3}}{\left[\left(Ab42^{oligo} + Ab42^{proto} + C_2 * Ab42^{plaque}\right)^{C_3} + C_4{}^{C_3}\right]} \qquad \textit{Equation 3}$$

2.2 Implementation of APOE4 genotypes

Building off the previous QSP Aβ aggregation model in APOE4 carriers and non-carriers with AD (36), we incorporated several intervention points for APOE4 genotypes (specifically, APOE4/4 and APOE3/4, vs. APOE3/3) in the amyloid cascade, including both Aβ synthesis from APP (43) and clearance by microglia (44). The parameter values for the different APOE genotypes are described in Results. The APOE genotype may also potentially affect the aggregation kinetics by directly binding of APOE protein to Aβ monomers and oligomers, particularly Aβ40 (45). Since the present analysis primarily focuses on the most pathogenic and aggregation-prone species Aβ42, we did not include this mechanism in the model.

2.3 Plasma p-tau calculation

Plasma p-tau changes were predicted from the dynamics of Aβ species using a multivariate regression approach (46). Briefly, 35 clinical data points were collected on plasma p-tau changes with the published anti-amyloid antibody therapies. The trajectories of Aβ oligomers, protofibrils and plaques were simulated using the appropriate clinical trial design for each of the studies. The correlation between the simulated dynamics of Aβ species and observed changes in plasma p-tau levels was the highest for Aβ42 protofibrils (r=0.79) and oligomers (r=0.74), followed by monomers (r=0.62), and finally plaques (r=0.22), suggesting that changes in plasma p-tau are driven by the more soluble Aβ species. The correlation between the observed plasma p-tau and the SUVR changes accounts for only 5% of the variability, while changes in soluble Aβ42 species can explain over 55% of the variability. A multivariate regression analysis using the simulated model outcomes can account for ~70% of the variability of p-tau changes (p=0.00029). Using this information, an equation linking plasma p-tau outcomes from a combination of different Aβ species was derived (46), which was then used to estimate the plasma p-tau levels based on the QSP predicted Aβ species changes.

2.4 Implementation of valiltramiprosate pharmacology

The primary MOA of valiltramiprosate is to impact Aβ aggregation by binding to Aβ monomers and preventing the formation of oligomers, i.e., enveloping conformational modification effect (31-34). Additionally, valiltramiprosate also acts as an APOE4 structure corrector that modifies APOE4 to an APOE3-like secondary conformation with functional properties of the APOE3 isoform (35). Figure 2 illustrates the QSP amyloid aggregation model components and the impact points where valiltramiprosate pharmacology was implemented.

The effect of valiltramiprosate on Aβ aggregation, in particular the forward rate constant k_f, was implemented using the following equation:

$$k_f = \left(1 - \left(\frac{[Drug]}{\left([Drug]+EC_{50}^{Drug}\right)}\right)\right) * k_f^0 \qquad \textit{Equation 4}$$

Where [Drug] is the drug concentration in brain ISF and k_f^0 is the default forward rate constant in the absence of the drug. This effect is implemented for both the primary (monomers binding to soluble oligomers) and secondary (monomers binding to oligomers on plaques) nucleation processes.

The APOE4 structure-corrector MOA of valiltramiprosate was implemented for several APOE4 specific mechanisms, assuming a complete phenotypic switch from APOE4/4 to APOE3/3. Valiltramiprosate affects microglia clearance parameters EC_{50} and V_{max} according to:

$$EC_{50} = EC_{50}^{APOE4/4} - \left(EC_{50}^{APOE4/4} - EC_{50}^{APOE3/3}\right) * \left(\frac{[Drug]}{\left([Drug]+EC_{50}^{Drug}\right)}\right) \qquad \textit{Equation 5}$$

And

$$V_{max} = V_{max}^{APOE4/4} + \left(V_{max}^{APOE3/3} - V_{max}^{APOE4/4}\right) * \left(\frac{[Drug]}{\left([Drug]+EC_{50}^{Drug}\right)}\right) \qquad \textit{Equation 6}$$

Also, valiltramiprosate affects the synthesis of Aβ peptides:

$$K_{in} = K_{in}^{APOE4/4} + \left(K_{in}^{APOE3/3} - K_{in}^{APOE4/4}\right) * \left(\frac{[Drug]}{\left([Drug]+EC_{50}^{Drug}\right)}\right) \qquad \textit{Equation 7}$$

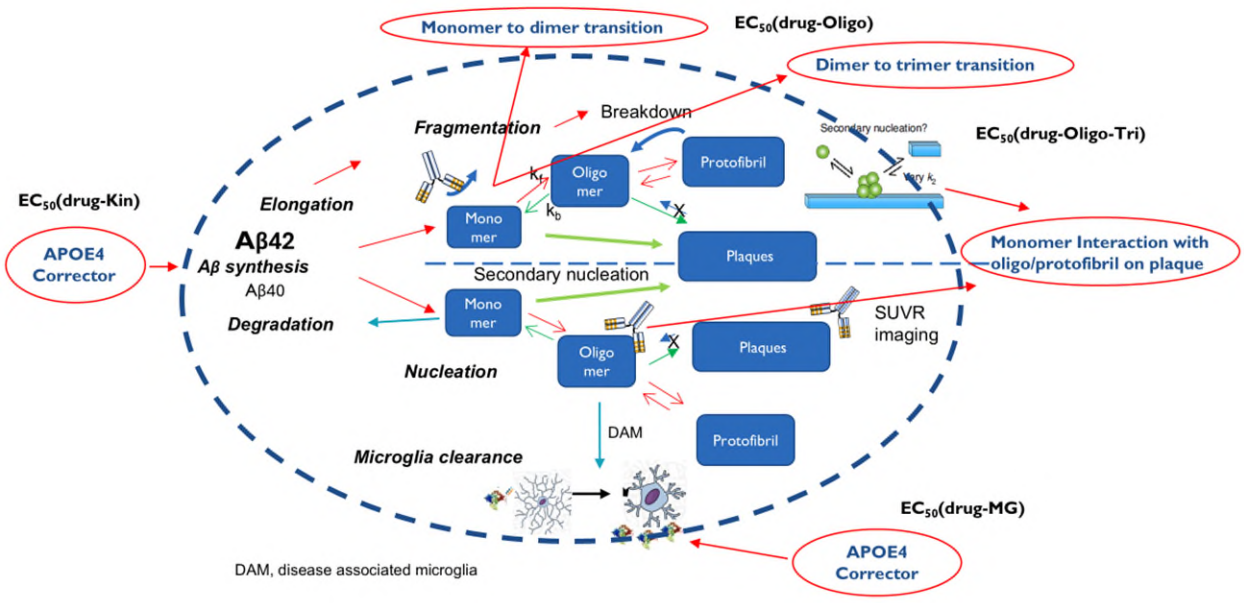


Figure 2. Schematic illustration of the mechanistic amyloid QSP model and valiltramiprosate pharmacology. *The QSP model includes Aβ42 and Aβ40 synthesis from the precursor protein APP, aggregation of monomers into oligomers, protofibrils and plaques, enzymatic degradation of monomers by insulin-degrading enzyme or neprilysin, and clearance of amyloid by microglia. The different Aβ species are defined as: monomers (n=1), oligomers (n=2-16) with molecular weights between 8 and 80 kDa, protofibrils (n=17-24) with molecular weights >80 kDa and plaques (n≥25). The impact of APOE genotype is applied as a differential effect on both Aβ clearance by microglia and Aβ production from APP. The pharmacology of valiltramiprosate is implemented as both an Aβ oligomer inhibitor and APOE4 structure corrector. Clinically relevant readouts include plasma Aβ42/Aβ40 ratio, CSF Aβ42, brain interstitial fluid soluble oligomers and protofibrils, SUVR, and plaque deposition. Aβ, β-amyloid; APOE, apolipoprotein E; APP, amyloid precursor protein; CSF, cerebro-spinal fluid; DAM, disease-associated microglia; QSP, quantitative systems pharmacology; SUVR, standardized uptake value ratio.*

2.5 Valiltramiprosate exposures in brain ISF

Valiltramiprosate levels in brain ISF were projected based on both the clinical PK and preclinical brain/plasma ratio data (Supplementary Data Figure S1). Previously, we reported the steady-state PK exposures in plasma following valiltramiprosate 265 mg *bis in die* (BID) at 2 weeks (Phase 1b study) and 65 weeks (Phase 2 study) in APOE4 carriers with early AD (30), which were comparable to that in the Phase 3 study (13). Following oral dosing, valiltramiprosate is rapidly converted to tramiprosate, which in turn is metabolized to 3-SPA. The plasma half-life is 1.4hr for the parent valiltramiprosate compared to 14.8hr and 37.5hr for tramiprosate and 3-SPA, respectively. Both tramiprosate and 3-SPA exhibit comparable Aβ anti-oligomer activities (31-33) and thus contributing equally to the clinical benefit. Both penetrate the brain with a combined steady-state brain/plasma AUC ratio ranging from 40% to >80% based on preclinical studies (24, 27). Thus, the steady-state brain ISF drug level for combined tramiprosate+3-SPA following valiltramiprosate 265mg BID dosing was projected to be approximately 2 μM (based on a 40% brain/plasma ratio) to 4 μM (based on an 80% brain/plasma ratio). This range of drug concentrations was used in the simulation.

2.6 Hippocampal volume trajectory model in AD

From the simulated Aβ species dynamics in the amyloid aggregation model, we calculated a readout for HV, based on the equation and factors listed below. In this study, we did not consider the potential asymmetry of left vs. right hippocampus, although there is evidence that APOE4 carriers may have a smaller left HV, but not right HV, compared to noncarriers (47).

$$\frac{HV(T_0+t)}{HV(T_0)} = 1 - \alpha(Age) * t - \beta\left(Ab_{path}(t)\right) - \gamma\left(\frac{Ab_{sol}(T_0+t)}{Ab_{sol}(T_0)}\right) + \delta\left(\frac{Ab_{pl}(T_0+t)}{Ab_{pl}(T_0)}\right) - \varepsilon * ARIA_E(t) + \theta * \frac{Microglia(T_0+t)}{Microglia(T_0)}$$

Equation 8

Age (coefficient α): Based on studies of age-dependent changes in HV in healthy volunteers (29, 48-51), we defined an APOE4 genotype-dependent change as a function of age. Because neuronal synapses contribute substantially to HV, the lower synapse density in APOE4 subjects provides a biological rationale (52). APOE4 is also associated with impaired hippocampal neurogenesis (53, 54).

Non-Aβ pathology (Ab_{path}, with coefficient β): This contribution accounts for other pathologies, including but not limited to tau and other co-pathologies like a-synuclein on HV (55), which is not affected by valiltramiprosate.

Soluble Aβ oligomers and protofibrils (Ab_{sol}, with coefficient γ): Since soluble Aβ oligomers directly affect neuronal survival, this is an important contribution to the protection of hippocampal atrophy for therapeutic agents that reduce Aβ oligomers, e.g., valiltramiprosate. These are experimentally inaccessible biomarkers that can only be simulated using QSP at this stage.

Amyloid plaque suburbia (Ab_{pl}, with coefficient δ): The beneficial sparing of HV by the anti-amyloid antibody-mediated reduction of soluble oligomers is compensated by the clearance of plaques (56). It has been suggested that increased removal and clearance of the plaques with anti-amyloid antibody therapies interferes with the ability to yield beneficial brain tissue preservation effects on vMRI due to the concept of pseudo-atrophy, a unique clinical feature of anti-amyloid antibodies (57). This negative interaction effect is not observed with valiltramiprosate (13, 14).

ARIA-E (ARIA$_E$, with coefficient ε): ARIA consists of ARIA-E (edematous) and ARIA-H (hemorrhagic) vascular abnormalities, driven by the migration of activated macrophages into perivascular spaces associated with fluid volume shifts leading to ventriculomegaly (56-59). These adverse events are associated with anti-amyloid antibody therapies, but not with valiltramiprosate (13, 14).

Microglia/astrocyte activation (coefficient θ): Reactive astrogliosis and microglia activation are associated with amyloid plaque deposition and are amplified by anti-amyloid antibodies (57, 60, 61). This effect on neuronal survival and brain volume is likely mediated by the release of pro-inflammatory cytokines (62).

Since we aimed to model the HV dynamics from a relatively healthy age all the way to the complete AD pathology, we defined an age transition or inflection point between the healthy trajectory and the onset of pathology (called Age$_{Infl}$). This transition function takes the following formula, where a is the quadratic coefficient and b is the linear coefficient:

$$MIN\left(1, a\left(age - Age_{infl}\right)^2 + b\left(age - Age_{infl}\right)\right) \qquad \textit{Equation 9}$$

With this function, this leads to the following equations for HV:

If age < Age$_{Infl}$

$$HV(age) = HV(age - 50) * \left(1 - \frac{\alpha + \beta}{4} * (Age - 50) - \frac{\gamma}{4} * \left(\frac{Ab_{sol}(age)}{Ab_{sol}(50)}\right) + \frac{\delta}{4}\left(\frac{Ab_{pl}(age)}{Ab_{pl}(50)}\right)\right)$$

Equation 10

Else

$$HV(age + \Delta t)$$

$$= HV(age) * (1 - (\alpha + \beta) * (\Delta t) * MIN\left(1, a(age - 55)^2 + b(age - 55)\right)$$

$$- \gamma \ * \Delta t \left(\frac{Ab_{sol}(age + \Delta t)}{Ab_{sol}(age)}\right) * MIN\left(1, a(age - 55)^2 + b(age - 55)\right) + \delta$$

$$* \Delta t \left(\frac{Ab_{pl}(age + \Delta t)}{Ab_{pl}(age)}\right) * MIN\left(1, a(age - 55)^2 + b(age - 55)\right) - \ \varepsilon$$

$$* \Delta t \left(\frac{ARIA_E(age + \Delta t)}{ARIA_E(age)}\right) * MIN\left(1, a(age - 55)^2 + b(age - 55)\right) + \theta$$

$$* \Delta t \left(\frac{Microglia(age + \Delta t)}{Microglia(age)}\right) * MIN\left(1, a(age - 55)^2 + b(age - 55)\right))$$

Equation 11

3. Results

3.1 Introduction of APOE4 genotypes into the amyloid aggregation model

It has been reported that APOE isoforms differentially affect APP transcription and Aβ secretion in neurons (43), and that APOE4 is associated with impaired Aβ uptake and clearance by microglia-like cells (44). We therefore incorporated APOE genotype-specific intervention points in the amyloid cascade, including both Aβ synthesis (reflected in the parameter K_{in}) and clearance (reflected in the parameters V_{max} and EC_{50}). The baseline parameter values for the different APOE genotypes are shown in Table 1, with the sensitivity analyses included in Supplementary Data Figures S2-S4.

Table 1. Parameter values for different APOE genotypes in the amyloid aggregation model.

APOE4 Allele	K_{in} (1/hr)	Microglia V_{max} (nM*hr)	Microglia EC_{50} (nM)
0	0.0125	0.000135	200
1	0.01275	0.000125	300
2	0.0145	0.000075	500

K_{in}, synthesis rate of Aβ from APP; V_{max}, maximal rate at which microglia can clear Aβ species; EC_{50}, Aβ species concentration for 50% of microglia-dependent clearance.

3.2 Natural trajectories of Aβ42 biomarkers by APOE4 genotype

Applying the parameters defined in Table 1, Figures 3&4 show the natural trajectories of plasma Aβ42/Aβ40 ratio, CSF Aβ42, brain ISF Aβ42 oligomers and protofibrils, and SUVR in generic APOE4/4, APOE3/4 and APOE3/3 AD patients. Overall, both plasma Aβ42/Aβ40 ratio and CSF Aβ42 deceased while brain Aβ42 oligomers, protofibrils and SUVR increased over time with the development and progression of AD. There were pronounced gene-dose differences in all these biomarkers indicative of disease acceleration, with a rank order of APOE4/4 >> APOE3/4 > APOE3/3. APOE4/4 exhibited a greater degree of acceleration in Aβ pathology compared to APOE3/4 and APOE 3/3, including a substantially earlier onset (i.e., leftward shift) and more rapid decline (plasma Aβ42/Aβ40 ratio and CSF Aβ42) or increase (brain Aβ42 oligomers, protofibrils and SUVR).

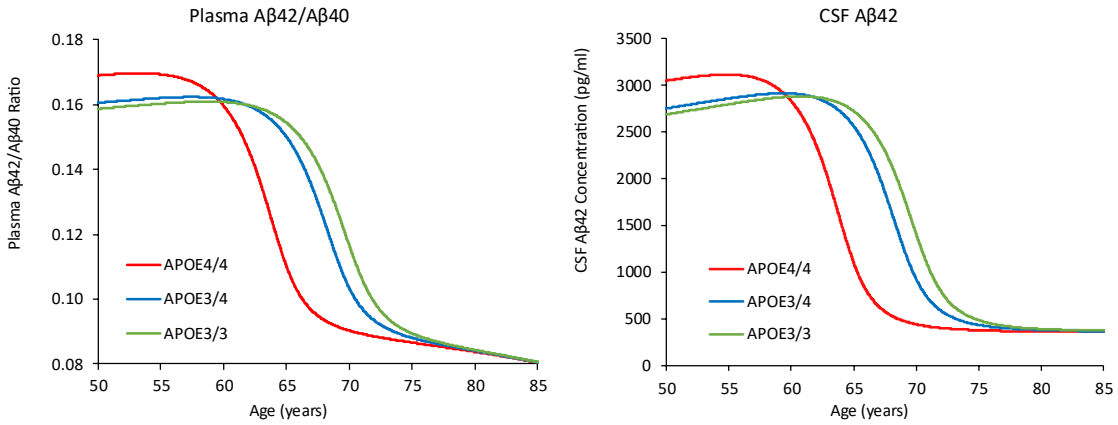


Figure 3. Natural trajectories of plasma Aβ42/Aβ40 ratio and CSF Aβ42 in APOE4/4, APOE3/4 and APOE3/3 AD patients. *Natural age-related amyloid pathology was implemented as a linear decrease in Aβ monomer degradation, resulting in a gradual increase of monomers into the aggregation pathway. A steep transition occurred at ~60 years of age with a rapid decline of plasma Aβ42/Aβ40 ratio and CSF Aβ42 with the development and progression of AD. The impact of APOE genotype was applied as a differential effect on both the clearance and production of Aβ. Aβ, β-amyloid; AD, Alzheimer's disease; APOE, apolipoprotein E; CSF, cerebro-spinal fluid; SUVR, standardized uptake value ratio.*

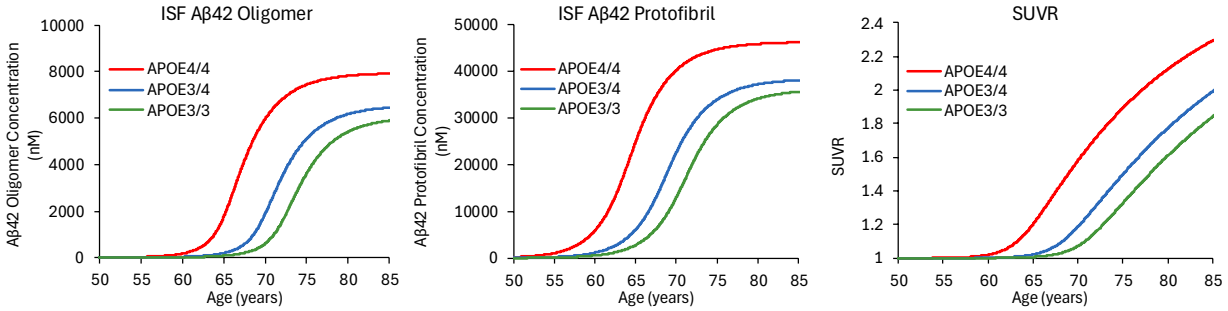


Figure 4. Natural trajectories of brain Aβ42 oligomer, protofibril and SUVR in APOE4/4, APOE3/4 and APOE3/3 AD patients. *A substantial increase of brain interstitial fluid Aβ oligomers, protofibrils and SUVR occurred at ~60 years of age with, which was followed by a plateau at older ages. This transition corresponded to the rapid decline of plasma Aβ42/Aβ40 ratio and CSF Aβ42 (see Figure 3) with the development and progression of AD. The impact of APOE genotype was applied as a differential effect on both the clearance and production of Aβ. Aβ, β-amyloid; AD, Alzheimer's disease; APOE, apolipoprotein E; CSF, cerebro-spinal fluid; SUVR, standardized uptake value ratio.*

3.3 Effects of valiltramiprosate on Aβ biomarkers by QSP analysis

We modeled the effects of valiltramiprosate 265mg BID treatment over 2 years on plasma Aβ42/Aβ40 ratio, CSF Aβ42, brain ISF Aβ42 oligomer+protofibril (the most neurotoxic species) and SUVR in generic APOE4/4, APOE3/4 and APOE3/3 AD patients, with the treatment initiation age from years 62 to 70. Figure 5 illustrates the effects when the treatment starts at age 65 and 70 years at a brain ISF drug exposure of 4 μM. Overall, valiltramiprosate increased plasma Aβ42/Aβ40 ratio and CSF Aβ42, decreased brain ISF oligomer+protofibril, and had a minimal effect on SUVR. This effect was seen across all three genotypes. Valiltramiprosate showed similar effects on soluble Aβ42 oligomers and protofibrils when examined separately. In agreement with these simulated data, we previously reported an elevation of plasma Aβ42/Aβ40 ratio and CSF Aβ42 in APOE4 carrier early AD subjects following 2-year valiltramiprosate 265mg BID in a Phase 2 biomarker study (28). Figure 6 shows that the Phase 2 trial plasma Aβ42/Aβ40 ratio changes in APOE3/4 and APOE4/4 early AD subjects after valiltramiprosate treatment were in good alignment with the QSP projections, providing validation for the model. The minimal effect on plaques, as reflected by the simulated SUVR, is consistent with the earlier finding that valiltramiprosate does not directly bind to amyloid plaques (24).

The monomer Aβ42 levels in both CSF and ISF were predicted to increase within the first week before reaching a stable plateau. The initial increase in monomer concentration was due to that valiltramiprosate blocked the forward rate constant, so that the continuously synthesized monomers were unable to bind to low-order aggregates. Valiltramiprosate reduced the synthesis of Aβ42 in APOE4/4 to a lower level equal to APOE3/3 via the APOE4 structure-corrector MOA. Furthermore, inhibition of amyloid aggregation by valiltramiprosate led to a reversal of the forward/backward rates, consequently the monomer dynamics became dominated by the reverse process, i.e., losing monomers from the already formed oligomers. This effect cascaded in the

whole sequence starting from the highest oligomer order working its way down with the biggest effect seen in the lower order oligomers.

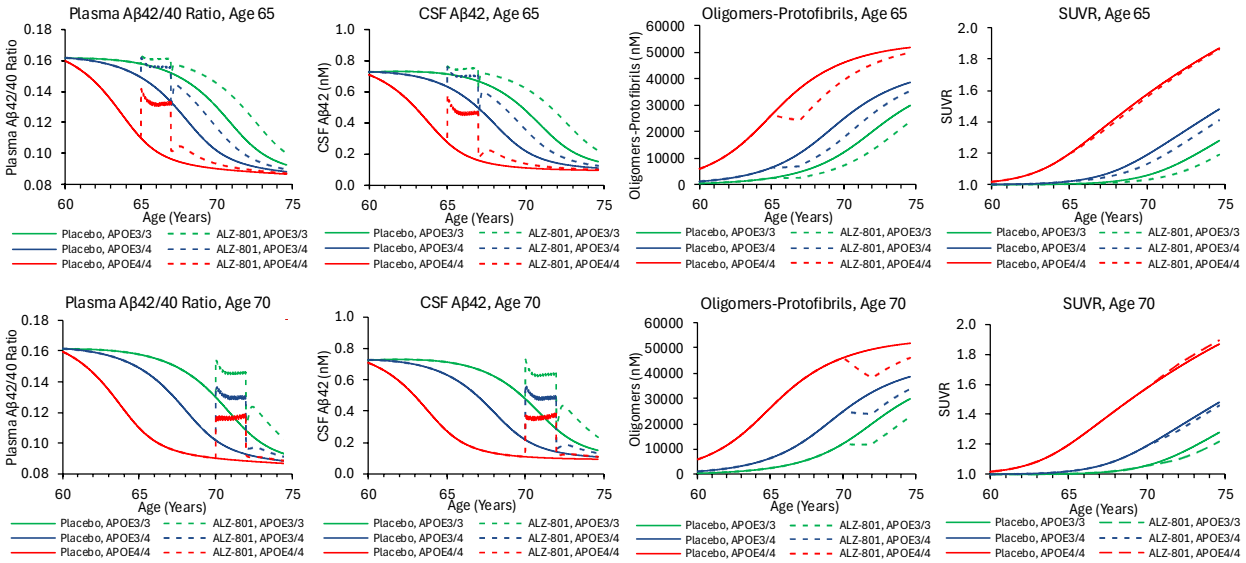


Figure 5. QSP-predicted effects on amyloid biomarkers following valiltramiprosate (ALZ-801) 265mg BID treatment over 2 years in APOE4/4, APOE3/4 and APOE3/3 AD patients. *Illustrated are the effects on plasma Aβ42/Aβ40 ratio, CSF Aβ42, brain interstitial fluid Aβ42 oligomer+protofibril (most neurotoxic species), and SUVR when the treatment was initiated at 65 and 70 years of age, with a brain interstitial fluid drug exposure of 4 μM at the steady state. Valiltramiprosate increased plasma Aβ42/Aβ40 ratio* and *CSF Aβ42 monomers, decreased brain Aβ42 oligomer+protofibril, and had a minimal effect on SUVR in all three APOE genotypes. The differences in treatment effect across the ages and genotypes are reflective of the stage of disease and the predose baseline amyloid pathology status. Valiltramiprosate's molecular mechanisms of action as both an Aβ oligomer inhibitor and an APOE4 structure corrector were implemented in the model. Aβ, β-amyloid; AD, Alzheimer's disease; APOE, apolipoprotein E; CSF, cerebro-spinal fluid; QSP, quantitative systems pharmacology; SUVR, standardized uptake value ratio.*

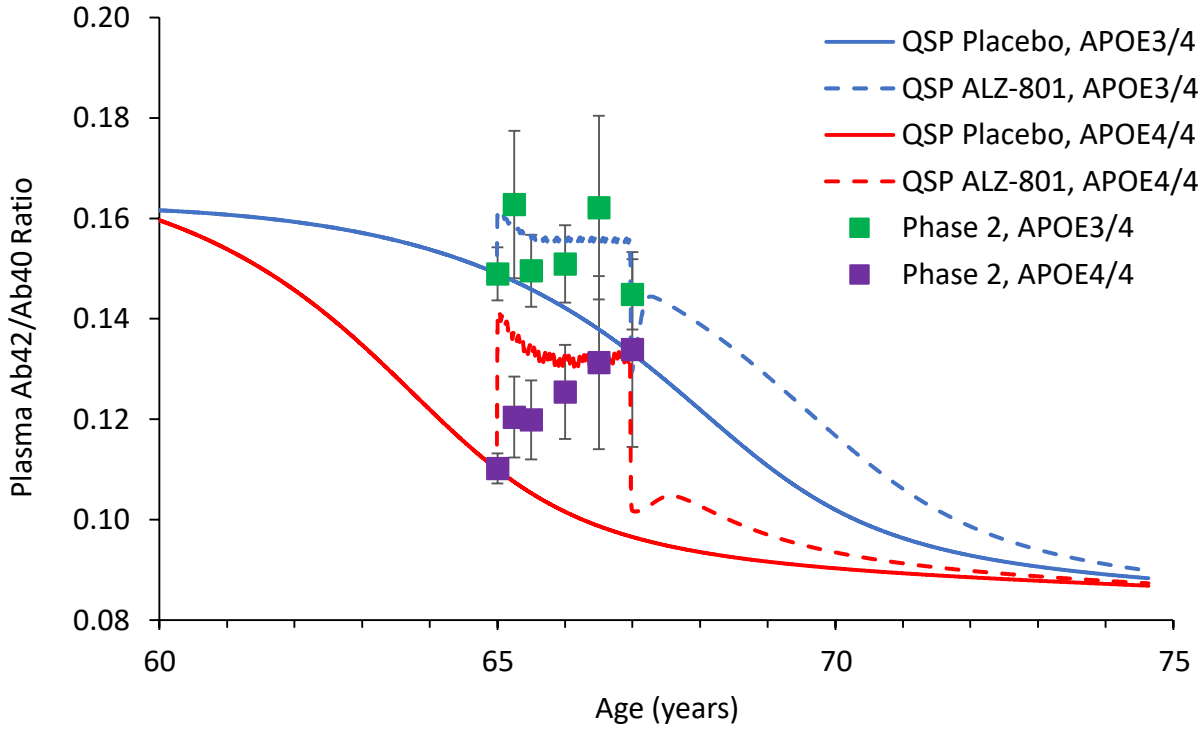


Figure 6. Comparison of the actual Phase 2 biomarker study data and the QSP-predicted plasma Aβ42/Aβ40 changes in APOE3/4 and APOE4/4 early AD subjects (average age 65) following valiltramiprosate (ALZ-801) 265mg BID treatment over 2 years. *The 104-week valiltramiprosate Phase 2 plasma Aβ42/Aβ40 ratio results in APOE4 carriers with early AD were previously published (28). Data from the APOE3/4 subjects (with an average age 65.2 years, range 53-69 years, n=30) and APOE4/4 subjects (with an average age 65.6 years, range 59-69 years, n=21) were summarized for comparison with the QSP-modeled changes at the treatment initiation age of 65 (Figure 5). The longitudinal Phase 2 plasma Aβ42/Aβ40 values (mean±SEM) as determined by an Euroimmun ELISA assay method (28) were converted to the scale of the QSP model based on the relative changes from baseline. The results show good agreement between the clinically observed and the QSP-predicted plasma Aβ42/Aβ40 ratio changes following 2-year*

valiltramiprosate 265mg BID treatment starting at age 65 in both APOE3/4 and APOE4/4 subjects with early AD. Aβ, β-amyloid; AD, Alzheimer's disease; APOE, apolipoprotein E; QSP, quantitative systems pharmacology.

Following treatment discontinuation, the forward rate constant returned back to baseline allowing the large concentration of monomers to be consumed in substantially more oligomers, explaining the large drop in CSF Aβ42. An increasing level of soluble oligomers allowed for more monomers to be formed in the backward reaction that might explain the secondary Aβ42 peak, observed at around 3 months. Afterwards, a slowly decreasing Aβ42 was observed to keep the monomer concentrations higher than the placebo level which took approximately 5-6 years to eventually reach the natural trajectory of the placebo. This block of the aggregation cascade during valiltramiprosate treatment reset the distribution of Aβ species so that the oligomers slowly returned to the level of the natural placebo trajectory with the same time dynamics. This process might take several years resulting in reduced oligomer-mediated neurotoxicity even after the treatment is stopped.

The results indicate that the beneficial effect of valiltramiprosate appeared to increase with the number of APOE4 alleles in combination with the age of treatment initiation. Valiltramiprosate either arrested or reversed the progressive increase of combined oligomer+protofibril vs. placebo in all APOE genotypes. The absolute decrease in combined oligomer+protofibril relative to placebo at the end of the treatment was larger in APOE4/4 due to the higher baseline levels at all treatment ages. The relative change from baseline was dependent on both age and genotype. At the age of 70, while the placebo levels increased between 7% (APOE4/4) and 63% (APOE3/3), simulated patients receiving treatment saw their oligomer+protofibril concentration decline by

18% (APOE4/4) and 3% (APOE3/3). The levels of protofibrils, calculated as the weighted average, decreased over time, with the AUC decreasing by 30-40% below the corresponding placebo values during treatment in all cases.

Additionally, a sensitivity analysis was performed to understand the relative contribution of valiltramiprosate's anti-Aβ oligomer vs. APOE4 structure-corrector MOA on Aβ biomarkers. Using brain Aβ42 protofibril levels as an example (Supplementary Data Figure S5), the simulation revealed a discernable effect of APOE4 structure-corrector mechanism, while the majority of the effect on protofibril reduction appeared to be due to the anti-Aβ oligomer MOA.

3.4 QSP-predicted reduction of plasma p-tau by valiltramiprosate

We projected the effect of valiltramiprosate on plasma p-tau levels (Figure 7) based on the QSP-modeled Aβ species changes. The results showed a consistent reduction in the natural elevation of plasma p-tau levels vs. placebo in all APOE genotypes and age of treatment initiation scenarios. When the treatment begins at the age of 67 and 70 years, a reduction in p-tau levels below the predose baseline was observed in APOE4/4 subjects.

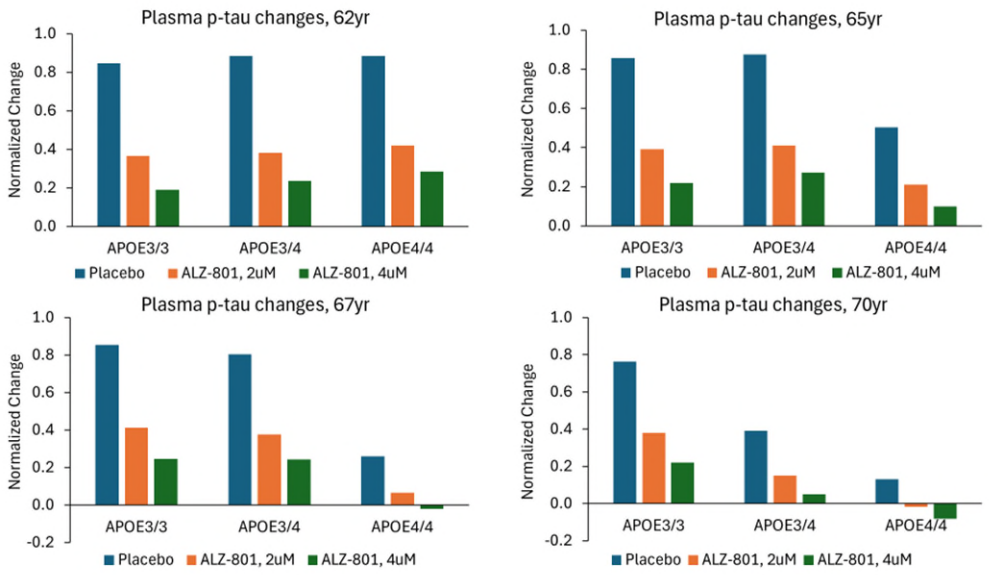


Figure 7. QSP-predicted reduction of plasma p-tau by valiltramiprosate in AD patients. *Plasma p-tau dynamics were simulated following 2-year valiltramiprosate 265mg BID treatment (predicted to produce 2-4 μM brain interstitial fluid drug exposures at the steady state) for different age, genotype and drug exposure scenarios. Normalized fold changes of plasma p-tau levels relative to baseline were projected from the QSP-simulated changes in Aβ42 species using the coefficients derived from a multivariate regression analysis as described in Methods. The results show consistent reductions in the natural elevation of plasma p-tau levels vs. placebo in all APOE genotypes and ages of treatment initiation, in an exposure-dependent manner. When valiltramiprosate treatment was initiated at 67 and 70 years of age, there was a reduction in p-tau levels below the predose baseline in APOE4/4 subjects. Aβ, β-amyloid; AD, Alzheimer's disease; APOE, apolipoprotein E; QSP, quantitative systems pharmacology.*

3.5 QSP analysis of long-term valiltramiprosate benefit in APOE4/4

We modeled generic APOE4/4 AD patients receiving continuous valiltramiprosate 265mg BID treatment over 10 years at the brain ISF drug exposures of 2-4 μM (Figure 8; Supplementary

Data Figures S6-S7). The results showed a substantial reduction of Aβ oligomers and protofibrils, which was dependent on the age of treatment initiation from 60 to 75 years and in an exposure-dependent manner. Consistent with this, there was a sustained, exposure-related elevation in CSF Aβ42 levels. The effect of valiltramiprosate on SUVR and plaques, while small in magnitude, was consistent with its MOA to inhibit Aβ oligomer formation thus leading to a small reduction on plaque formation that was dependent on early treatment initiation. Treatment initiation at either 70 or 75 years of age yielded negligible reduction in SUVR and plaque formation. Thus, valiltramiprosate is likely to produce a minimal plaque reduction in a mixed-age, early symptomatic AD population in short-term interventional trials, suggesting that this imaging biomarker is not a suitable endpoint for Aβ oligomer inhibitors like valiltramiprosate. The mechanism, however, is consistent with a small reduction in SUVR over chronic, long-term treatment (e.g., ≥ 5 years) due to the reduced amyloid deposition that occurs over time. In support, a reduction in plaque burden was observed following chronic tramiprosate treatment in an experimental transgenic murine model of AD, which is characterized by a phenotype of accelerated soluble and insoluble amyloid deposition and disease progression (24).

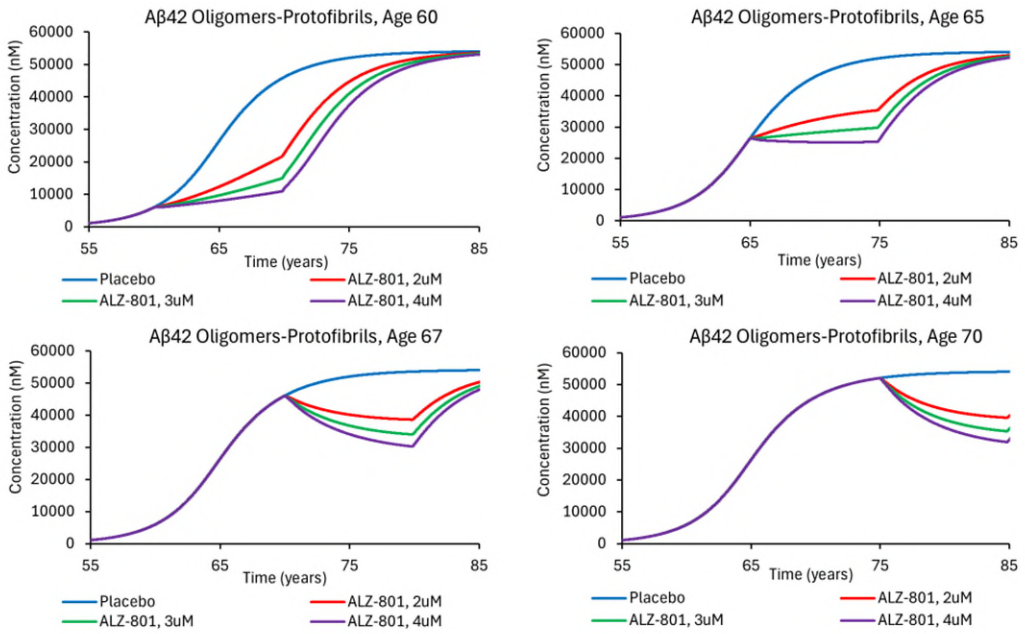


Figure 8. QSP-predicted long term valiltramiprosate benefit on combined brain Aβ42 oligomer+protofibril following 10-year 265mg BID treatment in APOE4/4 AD patients. *Illustrated are the simulated effects on brain interstitial fluid Aβ42 oligomer+protofibril (most neurotoxic species) when treatment was initiated at 60, 65, 70 and 75 years of age, with a steady-state brain interstitial fluid drug exposure ranging from 2 to 4 μM. Valiltramiprosate substantially reduced brain Aβ42 oligomer+protofibril in an age- and exposure-dependent manner. The earliest age of treatment initiation showed the greatest benefit, indicating that the long-term treatment efficacy is dependent on the stage of disease and the predose baseline amyloid pathology load. Aβ, β-amyloid; AD, Alzheimer's disease; APOE, apolipoprotein E; QSP, quantitative systems pharmacology.*

3.6 Hippocampal volume trajectories vs. amyloid trajectories in AD

We derived the HV changes in the independent variables for different APOE genotypes starting from the model readouts for the amyloid species, ARIA-E liability and microglia

activation. The longitudinal observational data (63, 64) and the placebo data from the lecanemab (10) and donanemab (11) interventional studies were used to calculate the relevant coefficients of these independent variables. For APOE4/4 and APOE3/4, we used the baseline HV data in the valiltramiprosate Phase 2 study (29). Adjusting the reported HV data to the model, we arrived at the coefficients in Table 2. Subsequently, the natural HV trajectories for the different APOE genotypes were projected.

Table 2. Parameter values for different APOE genotypes of the hippocampal atrophy trajectory model in AD.

Parameters	APOE3/3	APOE3/4	APOE4/4
Baseline volume (mm^3)	4255	4255	4215
Age - α	0.002	0.0055	0.01
Non-amyloid pathology - β	0.0024	0.0024	0.004
Amyloid oligomer - γ	0.045	0.045	0.045
Plaque suburbia - δ	0.003	0.003	0.003
ARIA-E - ε	0.39	0.39	0.39
Microglia-Astrocytosis - θ	0.006	0.006	0.006
Age for inflection specific atrophy (year)	55	55	54.3
Quadratic coefficient - a	0.0032	0.0032	0.0032
Linear coefficient - b	0.003	0.003	0.003

Values of the various coefficients in Equations 10 & 11 for the independent variables as different contributions to hippocampal volume calculations. Values reflect unilateral hippocampal volume.

Since there are limited natural trajectory data for the changes in amyloid species, microglia activity and ARIA-E in the literature, we calibrated the coefficients of these independent variables using the interventional studies with lecanemab (10) and donanemab (11). Only the lecanemab study reported that 15% of the subjects were APOE4/4 homozygotes, 60% were APOE3/4 heterozygotes and 25% were non-APOE4 carriers, while the donanemab study did not report the

individual percentages for the three genotypes. Based on these, we imputed a weighted average for the HV with 15% APOE4/4, 60% APOE3/4 and 25% APOE3/3 for calibration with lecanemab and donanemab. The model outcome generated changes in soluble oligomers/protofibrils, plaques, ARIA-E liability and microglia activation that predict the accessible amyloid biomarkers CSF Aβ42 and SUVR (36). Using these changes of the independent variables for an 18-month trial allowed us to define the remaining coefficients.

We compared the QSP-projected longitudinal trajectories for bilateral HV and plasma Aβ42/Aβ40 ratio in APOE4/4, APOE3/4 and APOE3/3 AD subjects (Figure 9). In both QSP models of HV and plasma Aβ42/Aβ40 ratio, there were pronounced genotype differences in disease progression indicative of acceleration, with APOE4/4 >> APOE3/4 > APOE3/3. The APOE4/4 genotype exhibited a much greater degree of disease acceleration in both Aβ pathology and hippocampal atrophy compared to APOE3/4 and APOE3/3, including an earlier onset, more rapid decline, and an earlier manifestation of pathologies prior to clinical and functional decline. The decline of plasma Aβ42/Aβ40 ratio in the APOE4/4 genotype also occurred at an earlier disease stage than the other two genotypes, and with a faster rate than HV, while also reaching the low plateau several years earlier than HV (65). The accelerated disease gene-dose effect was also observed with HV atrophy progression following the same rank order of APOE4/4 >> APOE3/4 > APOE3/3.

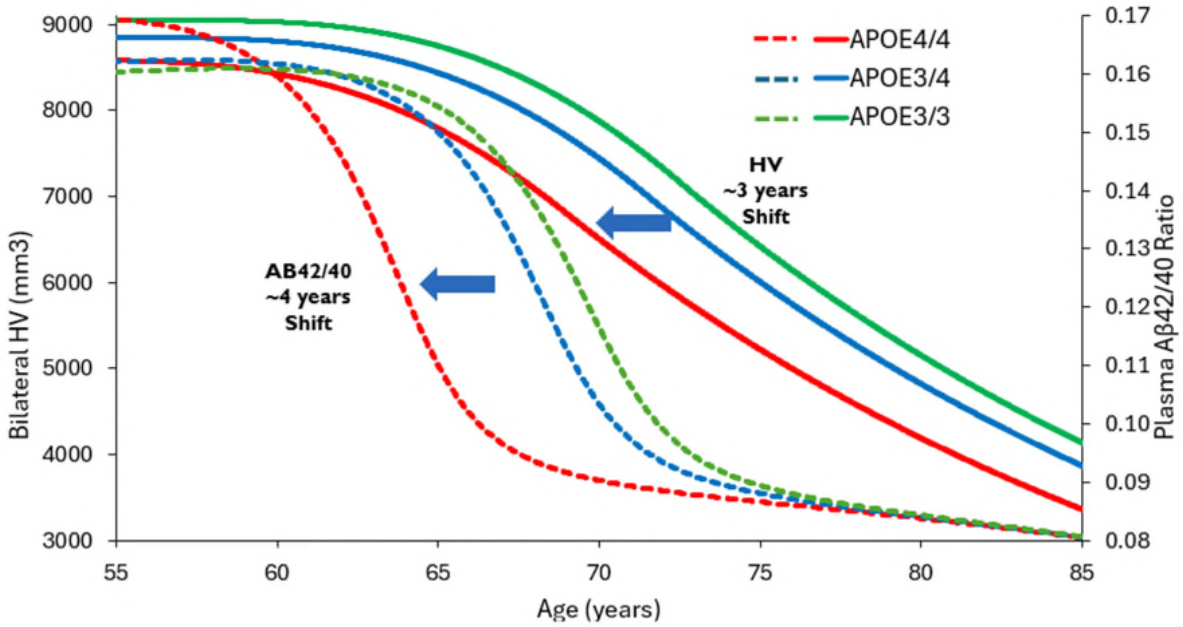


Figure 9. Comparison of the natural trajectories of bilateral hippocampal volume (HV) and plasma Aβ42/Aβ40 ratio in APOE4/4, APOE3/4 and APOE3/3 AD subjects. *The HV trajectories were developed based on the QSP amyloid aggregation model by integrating factors including age, non-Aβ pathology, Aβ species, ARIA-E, Aβ clearance and microglia activity. The impact of APOE genotype was applied as a differential effect on both Aβ clearance and production processes. The model coefficients were calibrated with the lecanemab and donanemab clinical trial data. The results show that changes of plasma Aβ42/Aβ40 ratio proceeded that of HV. In both QSP models of HV and plasma Aβ42/Aβ40 ratio, APOE genotype significantly influenced disease progression, with APOE4/4 linked to an earlier onset and faster Aβ pathology progression reflecting a gene-dose effect and aligning with clinical progression. Aβ, β-amyloid; AD, Alzheimer's disease; APOE, apolipoprotein E; ARIA-E, Amyloid-related Imaging Abnormalities (Edematous); HV, hippocampal volume; QSP, quantitative systems pharmacology.*

3.7 Comparison of valiltramiprosate Phase 3 hippocampal volume data vs. QSP-predicted natural trajectory model in APOE4/4 genotype

We compared the actual clinical HV outcomes from the valiltramiprosate Phase 3 trial (13) vs. the QSP-predicted natural HV trajectory in AD. The mean HV data following valiltramiprosate 265mg BID treatment over 78 weeks were fitted onto the QSP natural trajectory curve based on age. As shown in Figure 10, MCI subjects showed a better effect than Mild AD subjects after valiltramiprosate treatment. These results are consistent with the reported clinical findings from this study (13, 14).

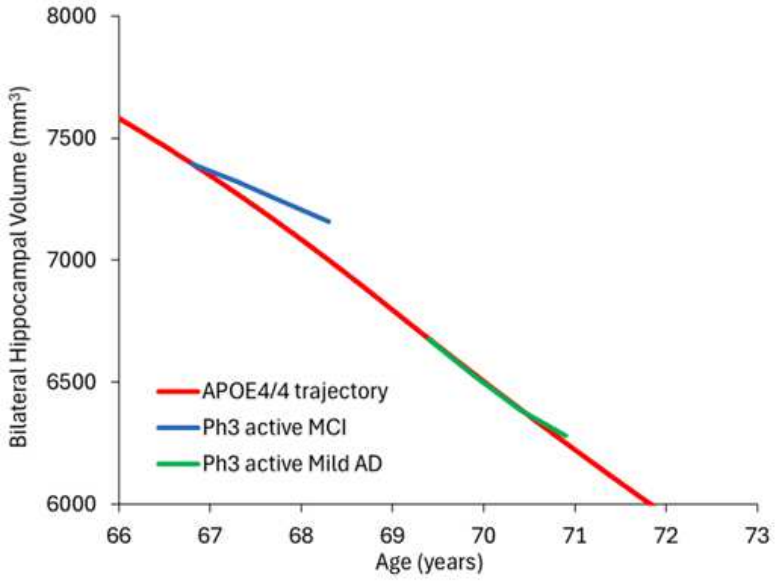


Figure 10. QSP hippocampal volume analysis confirms the observed reduction of bilateral hippocampal atrophy in MCI > Mild AD subjects in the valiltramiprosate Phase 3 study. *The observed mean longitudinal hippocampal volume data in APOE4/4 MCI and Mild AD subjects from the valiltramiprosate APOLLOE4 Phase 3 trial were modeled onto the QSP trajectory curve (red curve) based on age. The MCI subjects (blue curve) showed a reduced slope vs. the natural disease trajectory, while the Mild AD subjects (green color) showed minimal effect following 78*

weeks of valiltramiprosate 265mg BID treatment, consistent with the clinical observations. Aβ, β-amyloid; AD, Alzheimer's disease; APOE, apolipoprotein E; HV, hippocampal volume; QSP, quantitative systems pharmacology.

4. Discussion

This study expanded an established, well-calibrated mechanistic QSP model of Aβ aggregation in AD (36) to include APOE4 genotypes, specifically APOE4/4 and APOE3/4. APOE genotype-specific adjustments to parameters governing APP synthesis and microglia-mediated clearance of Aβ species were calibrated using longitudinal observational clinical data. We also developed a novel natural trajectory model of hippocampal atrophy, measured by hippocampal volume (HV), using observational and interventional datasets, including data from the CLARITY and TRAILBLAZER trials.

The QSP model reproduced marked APOE genotype-dependent differences in AD onset and progression across Aβ biomarkers, including the plasma Aβ42/Aβ40 ratio, CSF Aβ42, brain Aβ42 oligomers, protofibrils, SUVR, and HV. These differences followed a gene-dose pattern of APOE4/4 >> APOE3/4 > APOE3/3. Compared with APOE3/4 and APOE3/3, APOE4/4 showed faster Aβ pathology and hippocampal atrophy, earlier disease onset, more rapid decline, and earlier biomarker evidence of pathology before cognitive and functional symptoms emerged. Plasma Aβ42/Aβ40 ratio and CSF Aβ42 declined earlier in APOE4/4 subjects, progressed faster than hippocampal atrophy, and reached low plateau levels several years before healthy controls. This pattern supports a distinct, accelerated AD trajectory in APOE4/4 subjects (16). Accordingly, this APOE4 genotype-based QSP analysis supports the concept that accelerated amyloid aggregation,

reflected by rapid declines in plasma Aβ42/Aβ40 monomer ratio and CSF free Aβ42 fraction (28), is an early trigger for increased oligomer burden and plaque formation. These changes precede hippocampal atrophy and subsequent cognitive decline, indicating that APOE4/4 subjects represent a distinct population with faster HV atrophy that parallels Aβ aggregation biomarker dynamics.

The QSP HV trajectory model assumed that HV changes are driven by age, non-amyloid pathology, soluble oligomer and protofibril neurotoxicity, amyloid plaque volume, ARIA-E-related fluid shifts, and pro-inflammatory microglial activation. Age- and genotype-matched longitudinal ADNI data, together with lecanemab and donanemab interventional studies, were used to constrain APOE genotype-specific parameters while accounting for the pseudo-atrophy observed with anti-amyloid antibodies (57). Our results suggest that soluble Aβ oligomers and protofibrils are the primary drivers of HV atrophy, whereas plaque burden has minimal impact. Benefits from antibody-mediated reductions in oligomers and protofibrils appear to be largely offset by ARIA-E and microglial activation.

Valiltramiprosate is an oral anti-amyloid small-molecule prodrug that is rapidly converted in blood to tramiprosate and 3-SPA. Its primary mechanism is binding to Aβ monomers, thereby inhibiting toxic Aβ oligomer formation by preventing Aβ misfolding and aggregation, with an additional role as an APOE4 structure corrector (31-35). Based on preclinical animal data and human PK studies after 265 mg twice-daily oral dosing, brain ISF drug concentrations were estimated at 2-4 μM. Accordingly, the EC_{50} for valiltramiprosate's targets was conservatively set at 3 μM in this analysis.

The QSP model predicted that valiltramiprosate reduced soluble brain oligomer and protofibril levels by 25-30%. Although modest, this effect was amplified by the drug's position in

the aggregation cascade, substantially altering soluble oligomer and protofibril dynamics. These soluble Aβ aggregates are neurotoxic, cause neuronal loss and brain atrophy (6), and can induce neuronal hyperexcitability that directly impairs cognition (66). Consistent with this mechanism, the model predicted increases in plasma Aβ42/40 ratio and CSF Aβ42 after valiltramiprosate treatment, aligning with the prior findings in APOE4 carrier early AD subjects from a Phase 2 biomarker study (28). The similar plasma Aβ42/40 increases observed in that study and the modeled changes for APOE3/4 and APOE4/4 genotypes validated the present QSP model (Figure 6). Valiltramiprosate had little effect on SUVR or amyloid plaques, suggesting that amyloid imaging may not be a sensitive endpoint in standard 78- to 104-week AD interventional trials. Overall, valiltramiprosate effects were observed across all three genotypes and were exposure dependent.

Valiltramiprosate's effects on Aβ species depended on baseline levels, which vary by age, APOE genotype, and disease stage. By reducing the forward rate of Aβ monomer aggregation, the drug produced a complex redistribution of Aβ species. After treatment discontinuation, the full spectrum of Aβ species returned to natural AD trajectories over a mathematically predictable timeframe that depended on species, regimen, and disease stage. Notably, the QSP analysis showed that soluble oligomer and protofibril concentrations remained below placebo while monomer levels increased after valiltramiprosate treatment, indicating a favorable shift toward the monomeric state characteristic of normal, pre-disease physiology.

Long-term simulations indicated that, after chronic valiltramiprosate treatment was stopped, soluble oligomer and protofibril levels gradually returned to placebo trajectories within 6 to 8 years. These findings suggest that sustained long-term valiltramiprosate treatment is needed to maintain optimal clinical benefit in APOE4 carriers and non-carriers with amyloid-positive AD,

because disease progression resumes after discontinuation. Although the APOE4 structure-corrector mechanism produced a modest but measurable effect on brain Aβ biomarkers over two years, a larger effect may emerge with longer treatment as APOE4 shifts toward a healthier APOE3-like conformation, potentially producing delayed overall benefit.

Importantly, reducing soluble neurotoxic Aβ species with valiltramiprosate, and achieving early clinical benefit in AD, does not increase ARIA risk (13, 14). This is likely because valiltramiprosate does not interact with perivascular amyloid plaques or alter macrophage function. Consistent with this mechanism, safety data from the Phase 2 biomarker study (29) and the APOLLOE4 Phase 3 trial (13) showed no increase in ARIA among either APOE4/4 homozygotes or APOE3/4 heterozygotes.

The AD QSP model also reproduced the clinical finding that valiltramiprosate significantly preserves HV and appears to outperform anti-amyloid antibody therapies (9, 10, 13, 14, 29). This advantage likely reflects neuroprotection against Aβ oligomers and protofibrils without effects on plaque clearance, ARIA, or microglial activation. Comparison of Phase 3 HV data in APOE4/4 homozygotes with the QSP trajectory model showed reduced hippocampal atrophy primarily in MCI patients, consistent with clinical results (13, 14). Preservation of gray and white matter microstructure after valiltramiprosate treatment was previously confirmed by Diffusion Tensor Imaging (DTI) (13, 14). The model therefore helps predict disease stage-specific outcomes for individual patients. Because HV reflects neuronal integrity (67), its preservation is an important AD treatment goal, and earlier valiltramiprosate intervention may provide greater disease modification.

Using QSP-predicted Aβ species changes, we further projected valiltramiprosate's effect on plasma p-tau levels with a multivariate regression approach (46). The model predicted

consistent reductions in the natural rise of plasma p-tau vs. placebo across all APOE genotypes and treatment-initiation ages. When treatment started at ages 67 and 70, p-tau levels fell below predose baseline in APOE4/4 subjects. This projection aligns with our previously reported Phase 2 data showing statistically significant 27-43% reductions from baseline in plasma p-tau181 at all visits after valiltramiprosate 265 mg BID treatment in APOE4 carriers with a mean age of 69 years. Consistent with these findings, valiltramiprosate recently produced a significant reduction in plasma p-tau217 in both the overall early AD and MCI APOE4/4 populations in the APOLLOE4 Phase 3 trial. In MCI subjects, valiltramiprosate reduced plasma p-tau217 by 36% from baseline, whereas placebo increased it by 17%, yielding a sustained 53% drug-placebo difference over 78 weeks (68; manuscript in preparation). Thus, the current plasma p-tau projection, based on multivariate regression derived from available anti-amyloid antibody clinical data, may represent a conservative estimate of valiltramiprosate's observed clinical effects.

In this QSP study of valiltramiprosate pharmacology, an EC_{50} of 3 μM was used to model inhibition of Aβ oligomer formation, which may be conservative. A recent study (34) showed that valiltramiprosate prevented cytotoxicity from low-molecular-weight Aβ42 oligomers in cultured neuronal cells at a valiltramiprosate:Aβ42 stoichiometric ratio of 10:1, far below the 1000:1 ratio previously estimated from non-biological ion mobility spectrometry-mass spectrometry studies. Therefore, the actual treatment effect of valiltramiprosate may be greater than predicted by the present analysis.

In summary, this QSP analysis characterizes the natural progression of Aβ biomarkers and hippocampal volume in AD across APOE genotypes, demonstrating APOE4 gene dose-dependent disease acceleration according to the number of APOE4 alleles. Our findings highlight the ability of a well-calibrated QSP model to simulate therapeutic effects across clinically relevant scenarios

defined by age and APOE genotype, supporting more personalized treatment strategies. The results suggest that valiltramiprosate may provide clinical benefit by preventing formation of neurotoxic Aβ oligomers and protofibrils within the amyloid cascade, thereby reducing neurodegeneration, slowing clinical decline, and decelerating AD progression, with the greatest effects expected earlier in disease. These benefits were evident across all APOE genotypes evaluated, although their magnitude varied with amyloid pathology burden, age, genotype, disease stage, and timing of treatment initiation. Sustained oral valiltramiprosate therapy is also projected to exert disease-modifying effects on clinical and neurodegenerative endpoints without the ARIA risk associated with anti-amyloid antibody therapies.

Together, these findings suggest that the greatest clinical benefit may be achieved when oral valiltramiprosate is initiated early in amyloid pathogenesis, including during early symptomatic disease, with long-term treatment potentially preventing further progression if started at the presymptomatic stage. The clinical benefit observed in MCI subjects in the recently completed Phase 3 APOLLOE4 trial (13, 14) supports this conclusion.

Declarations:

Acknowledgments: The study and the publication of this paper were funded by Alzheon Inc.

Ethics approval and consent to participate: The APOLLOE4 trial was approved by Advarra Central IRB and by the required local university IRBs in the US, and by country specific Ethics Committees in UK and EU. The study was performed in accordance with the ethical standards as laid down in the 1964 Declaration of Helsinki and its later amendments or comparable ethical standards. All subjects and their partners, caregivers or legal representatives signed informed consent before participation in the APOLLOE4 trial.

Consent for publication: Not applicable.

Data Availability: The data and materials supporting the conclusions of this article are included within the article and its additional files.

Code Availability: The code used/generated during this study is not publicly available due to proprietary issues but may be available from the corresponding author on reasonable request.

Competing interests: JAH, JYY, JFS, SA, AP, and MT are employees of Alzheon, Inc. and receive salary compensations, stocks and/or stock options from Alzheon, Inc. HG, SMS and PVG are employees of Certara and compensated for services provided to Alzheon, Inc. and other companies.

Author's contributions: JAH, HG and JYY contributed to the manuscript preparation. JAH, JYY, JFS, HG and SMS contributed to the study design, data analysis and data interpretation. HG, SMS and PVG contributed to the QSP modeling. JAH, JYY, JFS, SA, AP and MT contributed to ALZ-801 Phase 3 clinical study design, conduct, data analysis and data interpretation. All authors reviewed the manuscript and approved the final version for publication.

References

1. Rajan KB, Weuve J, Barnes LL, McAninch EA, Wilson RS, Evans DA. Population estimate of people with clinical Alzheimer's disease and mild cognitive impairment in the United States (2020-2060). Alzheimers Dement 2021, 17(12):1966-75. doi: 10.1002/alz.12362.
2. Gustavsson A, Norton N, Fast T, Frölich L, Georges J, Holzapfel D, et al. Global estimates on the number of persons across the Alzheimer's disease continuum. Alzheimers Dement 2023, 19(2):658-70. doi: 10.1002/alz.12694.

3. Mufson EJ, Mahady L, Waters D, Counts SE, Perez SE, DeKosky ST, et al. Hippocampal plasticity during the progression of Alzheimer's disease. Neuroscience 2015, 309:51-67. doi: 10.1016/j.neuroscience.2015.03.006.
4. Tolar M, Abushakra S, Sabbagh M. The path forward in Alzheimer's disease therapeutics: Reevaluating the amyloid cascade hypothesis. Alzheimers Dement 2020, 16(11):1553-60. doi: 10.1016/j.jalz.2019.09.075.
5. Tolar M, Abushakra S, Hey JA, Porsteinsson A, Sabbagh M. Aducanumab, gantenerumab, BAN2401, and ALZ-801 - the first wave of amyloid-targeting drugs for Alzheimer's disease with potential for near term approval. Alzheimers Res Ther 2020, 12(1):95. doi: 10.1186/s13195-020-00663-w.
6. Lublin AL, Gandy S. Amyloid-beta oligomers: possible roles as key neurotoxins in Alzheimer's Disease. Mt Sinai J Med 2010, 77(1):43-9. doi: 10.1002/msj.20160.
7. Tolar M, Hey J, Power A, Abushakra S. Neurotoxic soluble amyloid oligomers drive Alzheimer's pathogenesis and represent a clinically validated target for slowing disease progression. Int J Mol Sci 2021, 22:6355. doi: 10.3390/ijms22126355.
8. Tolar M, Hey JA, Power A, Abushakra S. The single toxin origin of Alzheimer's disease and other neurodegenerative disorders enables targeted approach to treatment and prevention. Int J Mol Sci 2024, 25(5):2727. doi: 10.3390/ijms25052727.
9. Budd Haeberlein S, Aisen PS, Barkhof F, Chalkias S, Chen T, Cohen S, et al. Two randomized Phase 3 studies of aducanumab in early Alzheimer's disease. J Prev Alzheimers Dis 2022, 9(2):197-210. doi: 10.14283/jpad.2022.30.
10. van Dyck CH, Swanson CJ, Aisen P, Bateman RJ, Chen C, Gee M, et al. Lecanemab in early Alzheimer's disease. N Engl J Med 2023, 388(1):9-21. doi: 10.1056/NEJMoa2212948.

11. Sims JR, Zimmer JA, Evans CD, Lu M, Ardayfio P, Sparks J, et al. Donanemab in early symptomatic Alzheimer disease: The TRAILBLAZER-ALZ 2 randomized clinical trial. JAMA 2023, 330(6):512-27. doi: 10.1001/jama.2023.13239.
12. Abushakra S, Porsteinsson AP, Sabbagh M, Watson D, Power A, Liang E, et al. APOLLOE4 Phase 3 study of oral ALZ-801/valiltramiprosate in APOE ε4/ε4 homozygotes with early Alzheimer's disease: trial design and baseline characteristics. Alzheimers Dement (N Y) 2024, 10(3):e12498. doi: 10.1002/trc2.12498.
13. Abushakra S, Power A, Watson D, Porsteinsson A, Sabbagh M, MacSweeney E, et al. Clinical efficacy, safety and imaging effects of oral valiltramiprosate in APOEε4/ε4 homozygotes with early Alzheimer's disease: results of the Phase III, randomized, double-blind, placebo-controlled, 78-week APOLLOE4 trial. Drugs 2025, 85(11):1455-72. doi: 10.1007/s40265-025-02250-5.
14. Abushakra S, Doraiswamy PM, Hey JA, Tosun D, Barkhof F, Barakos J, et al. Hippocampal atrophy on magnetic resonance imaging as a surrogate marker for clinical benefit and neurodegeneration in early symptomatic Alzheimer's disease: synthesis of evidence from observational and interventional trials. CNS Drugs 2025, Dec 1. doi: 10.1007/s40263-025-01251-y. Online ahead of print.
15. Reiman EM, Arboleda-Velasquez JF, Quiroz YT, Huentelman MJ, Beach TG, Caselli RJ, et al. Exceptionally low likelihood of Alzheimer's dementia in APOE2 homozygotes from a 5,000-person neuropathological study. Nat Commun 2020, 11(1):667. doi: 10.1038/s41467-019-14279-8.

16. Fortea J, Pegueroles J, Alcolea D, Belbin O, Dols-Icardo O, Vaqué-Alcázar L, et al. APOE4 homozygozity represents a distinct genetic form of Alzheimer's disease. Nat Med 2024, 30(5):1284-91. doi: 10.1038/s41591-024-02931-w.
17. Blacker D, Haines JL, Rodes L, Terwedow H, Go RC, Harrell LE, et al. ApoE-4 and age at onset of Alzheimer's disease: the NIMH genetics initiative. Neurology 1997, 48(1):139-47. doi: 10.1212/wnl.48.1.139.
18. Jack CR Jr, Petersen RC, Xu Y, O'Brien PC, Smith GE, Ivnik RJ, et al. Rates of hippocampal atrophy correlate with change in clinical status in aging and AD. Neurology 2000, 55(4):484-89. doi: 10.1212/wnl.55.4.484.
19. Petersen RC, Aisen PS, Beckett LA, Donohue MC, Gamst AC, Harvey DJ, et al. Alzheimer's Disease Neuroimaging Initiative (ADNI): clinical characterization. Neurology 2010;74(3):201-9. doi: 10.1212/WNL.0b013e3181cb3e25.
20. European Medicines Agency. Qualification opinion of low hippocampal volume (atrophy) by MRI for use in regulatory clinical trials in pre-dementia stage of Alzheimer's disease, 2011.
21. Hill DLG, Schwarz AJ, Isaac M, Pani L, Vamvakas S, Hemmings R, et al. Coalition Against Major Diseases/European Medicines Agency biomarker qualification of hippocampal volume for enrichment of clinical trials in predementia stages of Alzheimer's disease. Alzheimers Dement 2014, 10(4):421-29.e3. doi: 10.1016/j.jalz.2013.07.003.
22. European Medicines Agency (EMA) guideline on the clinical investigation of medicines for the treatment of Alzheimer's disease, 2018.
23. Jack CR Jr, Bennett DA, Blennow K, Carrillo MC, Feldman HH, Frisoni GB, et al. A/T/N: An unbiased descriptive classification scheme for Alzheimer disease biomarkers. Neurology 2016, 87(5):539-47. doi: 10.1212/WNL.0000000000002923.

24. Gervais F, Paquette J, Morissette C, Krzywkowski P, Yu M, Azzi M, et al. Targeting soluble Abeta peptide with Tramiprosate for the treatment of brain amyloidosis. Neurobiol Aging 2007, 28(4):537-47. doi: 10.1016/j.neurobiolaging.2006.02.015.

25. Abushakra S, Porsteinsson A, Vellas B, Cummings J, Gauthier S, Hey JA, et al. Clinical benefits of tramiprosate in Alzheimer's disease are associated with higher number of APOE4 alleles: the 'APOE4 gene-dose effect'. J Prev Alzheimers Dis 2016, 3(4):219-28. doi: 10.14283/jpad.2016.115.

26. Abushakra S, Porsteinsson A, Scheltens P, Sadowsky C, Vellas B, Cummings J, et al. Clinical effects of tramiprosate in APOE4/4 homozygous patients with mild Alzheimer's disease suggest disease modification potential. J Prev Alzheimers Dis 2017, 4(3):149-56. doi: 10.14283/jpad.2017.26.

27. Hey JA, Yu JY, Versavel M, Abushakra S, Kocis P, Power A, et al. Clinical pharmacokinetics and safety of ALZ-801, a novel prodrug of tramiprosate in development for the treatment of Alzheimer's disease. Clin Pharmacokinet 2018, 57(3):315-33. doi: 10.1007/s40262-017-0608-3.

28. Hey JA, Yu JY, Abushakra S, Schaefer JF, Power A, Kesslak P, et al. Analysis of cerebrospinal fluid, plasma β-amyloid biomarkers, and cognition from a 2-year Phase 2 trial evaluating oral ALZ-801/Valiltramiprosate in APOE4 carriers with early Alzheimer's disease using quantitative systems pharmacology model. Drugs 2024, 84(7):825-39. doi: 10.1007/s40265-024-02068-7.

29. Hey JA, Abushakra S, Blennow K, Reiman EM, Hort J, Prins ND, et al. Effects of oral ALZ-801/Valiltramiprosate on plasma biomarkers, brain hippocampal volume, and cognition:

results of 2-year single-arm, open-label, Phase 2 trial in APOE4 carriers with early Alzheimer's disease. Drugs 2024, 84(7):811-23. doi: 10.1007/s40265-024-02067-8.

30. Hey JA, Yu JY, Abushakra S, Schaefer JF, Power A, Kesslak P, et al. Clinical pharmacokinetics of oral ALZ-801/Valiltramiprosate in a 2-year Phase 2 trial of APOE4 carriers with early Alzheimer's disease. Clin Pharmacokinet 2025, 64(3):407-24. doi: 10.1007/s40262-025-01482-8.
31. Hey JA, Kocis P, Hort J, Abushakra S, Power A, Vyhnálek M, et al. Discovery and identification of an endogenous metabolite of tramiprosate and its prodrug ALZ-801 that inhibits beta amyloid oligomer formation in the human brain. CNS Drugs 2018, 32(9):849-61. doi: 10.1007/s40263-018-0554-0.
32. Kocis P, Tolar M, Yu J, Sinko W, Ray S, Blennow K, et al. Elucidating the Aβ42 anti-aggregation mechanism of action of tramiprosate in Alzheimer's disease: integrating molecular analytical methods, pharmacokinetic and clinical data. CNS Drugs 2017, 31(6):495-509. doi: 10.1007/s40263-017-0434-z.
33. Liang C, Savinov SN, Fejzo J, Eyles SJ, Chen J. Modulation of amyloid-β42 conformation by small molecules through nonspecific binding. J Chem Theory Comput 2019, 15(10):5169-74. doi: 10.1021/acs.jctc.9b00599.
34. Muramatsu D, Watanabe-Nakayama T, Tsuji M, Umeda K, Hikishima S, Nakano H, et al. ALZ-801 prevents amyloid beta-protein assembly and reduces cytotoxicity: a preclinical experimental study. FASEB J 2025, 39(3):e70382. doi: 10.1096/fj.202402622R.
35. Nemergut M, Marques SM, Uhrik L, Vanova T, Nezvedova M, Gadara DC, et al. Domino-like effect of C112R mutation on ApoE4 aggregation and its reduction by Alzheimer's Disease drug candidate. Mol Neurodegener 2023, 18(1):38. doi: 10.1186/s13024-023-00620-9.

36. Geerts H, Walker M, Rose R, Bergeler S, van der Graaf PH, Schuck E, et al. A combined physiologically-based pharmacokinetic and quantitative systems pharmacology model for modeling amyloid aggregation in Alzheimer's disease. CPT Pharmacometrics Syst Pharmacol 2023, 12(4):444-61. doi: 10.1002/psp4.12912.
37. Geerts H, Bergeler S, Walker M, Rose R, Van der Graaf P. Exploring treatment guidelines for amyloid therapies in Alzheimer's disease using predictive quantitative system pharmacology modeling. Alzheimers Dement 2023, 19(Suppl. 24):e082487. doi:10.1002/alz.082487.
38. Lannfelt L, Johannesson M, Nygren P, Söderberg L, Möller C. Binding profiles to different amyloid-beta species of lecanemab, aducanumab and gantenerumab, the three most developed antibodies for Alzheimer's disease. J Prev Alzheimers Dis 2021, 8, Suppl 1.
39. Bassendine MF, Taylor-Robinson SD, Fertleman M, Khan M, Neely D. Is Alzheimer's disease a liver disease of the brain? J Alzheimers Dis 2020, 75(1):1-14. doi: 10.3233/JAD-190848.
40. Zetterberg H, Blennow K, Hanse E. Amyloid beta and APP as biomarkers for Alzheimer's disease. Exp Gerontol 2010, 45(1):23-9. doi: 10.1016/j.exger.2009.08.002.
41. Beach TG, Maarouf CL, Intorcia A, Sue LI, Serrano GE, Lu M, et al. Antemortem-postmortem correlation of Florbetapir (18F) PET amyloid imaging with quantitative biochemical measures of Aβ42 but not Aβ40. J Alzheimers Dis 2018, 61(4):1509-16. doi: 10.3233/JAD-170762.
42. Klunk WE, Koeppe RA, Price JC, Benzinger TL, Devous MD Sr, Jagust WJ, et al. The Centiloid Project: standardizing quantitative amyloid plaque estimation by PET. Alzheimers Dement 2015, 11(1):1-15.e1-4. doi: 10.1016/j.jalz.2014.07.003.
43. Huang YA, Zhou B, Wernig M, Südhof TC. ApoE2, ApoE3, and ApoE4 differentially stimulate APP transcription and Aβ secretion. Cell 2017, 168(3):427-41.e21. doi: 10.1016/j.cell.2016.12.044.

44. Lin YT, Seo J, Gao F, Feldman HM, Wen HL, Penney J, et al. APOE4 causes widespread molecular and cellular alterations associated with Alzheimer's disease phenotypes in human iPSC-derived brain cell types. Neuron 2018, 98(6):1141-54.e7. doi: 10.1016/j.neuron.2018.05.008.
45. Ghosh S, Sil TB, Dolai S, Garai K. High-affinity multivalent interactions between apolipoprotein E and the oligomers of amyloid-β. FEBS J 2019, 286(23):4737-53. doi: 10.1111/febs.14988.
46. Geerts H, Short SM, Grant A, van der Graaf PH. Understanding quantitative effects of anti-amyloid therapies on tau biomarkers and functional outcome. Insights from a comprehensive mechanistic quantitative systems pharmacology study. Front Pharmacol 2026, 17:1813290. doi: 10.3389/fphar.2026.1813290.
47. Pievani M, Galluzzi S, Thompson PM, Rasser PE, Bonetti M, Frisoni GB. APOE4 is associated with greater atrophy of the hippocampal formation in Alzheimer's disease. Neuroimage 2011, 55(3), 909-19. doi: 10.1016/j.neuroimage.2010.12.081.
48. Abushakra S, Porsteinsson AP, Sabbagh M, Bracoud L, Schaerer J, Power A, et al. APOE ε4/ε4 homozygotes with early Alzheimer's disease show accelerated hippocampal atrophy and cortical thinning that correlates with cognitive decline. Alzheimers Dement (N Y) 2020, 6(1):e12117. doi: 10.1002/trc2.12117.
49. Baumeister H, Vogel JW, Insel PS, Kleineidam L, Wolfsgruber S, Stark M, et al. A generalizable data-driven model of atrophy heterogeneity and progression in memory clinic settings. Brain 2024, 147(7):2400-13. doi: 10.1093/brain/awae118.
50. Frisoni GB, Fox NC, Jack CR Jr, Scheltens P, Thompson PM. The clinical use of structural MRI in Alzheimer disease. Nat Rev Neurol 2010, 6(2):67-77. doi: 10.1038/nrneurol.2009.215.

51. Gao N, Ye C, Chen H, Hao X, Ma T. MRI-based axis-referenced morphometric model corresponding to lamellar organization for assessing hippocampal atrophy in dementia. Hum Brain Mapp 2024, 45(10):e26715. doi: 10.1002/hbm.26715.
52. He K, Li B, Wang J, Wang Y, You Z, Chen X, et al. APOE ε4 is associated with decreased synaptic density in cognitively impaired participants. Alzheimers Dement 2024, 20(5), 3157-66. doi: 10.1002/alz.13775.
53. Tensaouti Y, Stephanz EP, Yu TS, Kernie SG. ApoE regulates the development of adult newborn hippocampal neurons. eNeuro 2018, 5(4), ENEURO.0155-18.2018. doi: 10.1523/ENEURO.0155-18.2018.
54. Meyer-Acosta KK, Diaz-Guerra E, Varma P, Aruk A, Mirsadeghi S, Muniz-Perez A, et al. APOE4 impacts cortical neurodevelopment and alters network formation in human brain organoids. Stem Cell Reports 2025, 20(7), 102537. doi: 10.1016/j.stemcr.2025.102537.
55. Fujishima M, Kawasaki Y, Mitsuhashi T, Matsuda H; Alzheimer's Disease Neuroimaging Initiative. Impact of amyloid and tau positivity on longitudinal brain atrophy in cognitively normal individuals. Alzheimers Res Ther 2024, 16(1):77. doi: 10.1186/s13195-024-01450-7.
56. Alves F, Kalinowski P, Ayton S. Accelerated brain volume loss caused by anti-β-amyloid drugs: a systematic review and meta-analysis. Neurology 2023, 100(20):e2114-24. doi: 10.1212/WNL.0000000000207156.
57. Belder CRS, Boche D, Nicoll JAR, Jaunmuktane Z, Zetterberg H, Schott JM, et al. Brain volume change following anti-amyloid β immunotherapy for Alzheimer's disease: amyloid-removal-related pseudo-atrophy. Lancet Neurol 2024, 23(10):1025-34. doi: 10.1016/S1474-4422(24)00335-1.

58. Barkhof F, Knopman DS. Brain shrinkage in anti-β-amyloid Alzheimer trials: neurodegeneration or pseudoatrophy? Neurology 2023, 100(20):941-42. doi: 10.1212/WNL.0000000000207268.
59. Hampel H, Elhage A, Cho M, Nicoll JA, Atri A. Amyloid-related imaging abnormalities (ARIA) and their radiological, biological and clinical characteristics: a plain language summary. Neurodegener Dis Manag 2024, 14(3-4):51-62. doi: 10.1080/17582024.2024.2343539.
60. De Strooper B, Karran E. The cellular phase of Alzheimer's disease. Cell 2016, 164(4):603-15. doi: 10.1016/j.cell.2015.12.056.
61. Franco-Bocanegra DK, Gourari Y, McAuley C, Chatelet DS, Johnston DA, Nicoll JAR, et al. Microglial morphology in Alzheimer's disease and after Aβ immunotherapy. Sci Rep 2021, 11(1):15955. doi: 10.1038/s41598-021-95535-0.
62. Verri M, Pastoris O, Dossena M, Aquilani R, Guerriero F, Cuzzoni G, et al. Mitochondrial alterations, oxidative stress and neuroinflammation in Alzheimer's disease. Int J Immunopathol Pharmacol 2012, 25(2):345-53. doi: 10.1177/039463201202500204.
63. Soldan A, Wang J, Pettigrew C, Davatzikos C, Erus G, Hohman TJ, et al. Alzheimer's disease genetic risk and changes in brain atrophy and white matter hyperintensities in cognitively unimpaired adults. Brain Commun 2024, 6(5):fcae276. doi: 10.1093/braincomms/fcae276.
64. Veldsman M, Nobis L, Alfaro-Almagro F, Manohar S, Husain M. The human hippocampus and its subfield volumes across age, sex and APOE e4 status. Brain Commun 2020, 3(1):fcaa219. doi: 10.1093/braincomms/fcaa219.

65. Peskind ER, Li G, Shofer J, Quinn JF, Kaye JA, Clark CM, et al. Age and apolipoprotein E*4 allele effects on cerebrospinal fluid beta-amyloid 42 in adults with normal cognition. Arch Neurol 2006, 63(7):936-9. doi: 10.1001/archneur.63.7.936.

66. Min-Kaung-Wint-Mon, Kida H, Kanehisa I, Kurose M, Ishikawa J, Sakimoto Y, et al. Adverse effects of Aβ1-42 oligomers: impaired contextual memory and altered intrinsic properties of CA1 pyramidal neurons. Biomolecules 2024, 14(11):1425. doi: 10.3390/biom14111425.

67. Simić G, Kostović I, Winblad B, Bogdanović N. Volume and number of neurons of the human hippocampal formation in normal aging and Alzheimer's disease. J Comp Neurol 1997, 379(4):482-94. doi: 10.1002/(sici)1096-9861(19970324)379:4<482::aid-cne2>3.0.co;2-z.

68. Hey JA, Abushakra S, Liang E, Yu J, Kesslak P, Bray M, et al. Valiltramiprosate on plasma p-tau217, p-tau217/Aβ42, vMRI and clinical correlations in Phase 3 APOE4/4 early AD subjects. AAIC abstract #10492, London, July 2026.

Supplementary Files

This is a list of supplementary files associated with this preprint. Click to download.

- QSPSupplementaryDataS1702AUG2026final.docx